

OXYGEN ION IMPURITY IN THE TEXTOR-94 BOUNDARY PLASMA OBSERVED BY ZEEMAN SPECTROSCOPY

J. D. Hey¶, C. C. Chu¶, S. Brezinsek‡, E. Hintz‡, Ph. Mertens‡, D. Rusbüldt‡, U. Samm‡,
and B. Unterberg‡

¶ Plasma Physics Research Institute, University of Natal, Durban 4041, South Africa
(hey@nu.ac.za, chu@nu.ac.za)

‡ Institut für Plasmaphysik, Forschungszentrum Jülich GmbH, D-52425 Jülich, Germany
(ph.mertens@fz-juelich.de)

1. Introduction and experimental method

Species identification by Zeeman spectroscopy offers unique advantages for tokamak boundary plasma studies, because of the detailed structure contained in multiplet transitions strongly perturbed by the Paschen-Back effect [1]. Charge-exchange recombination (CXR) spectroscopy for accurate ion temperature determination depends on the assumption, that the measured spectrum is not contaminated by unknown sources of line radiation. However, because spectral lines from high principal quantum numbers in H-like, He-like, or Li-like ions are usually selected, radiator states with low azimuthal (ℓ) quantum numbers make a minor contribution to the profiles. Thus, impurity contributions to these profiles may be hard to recognise [2,3]. For example, consider the species oxygen, which has a radiation potential roughly 3 times that of carbon [4,5]. Since high $n-\alpha$ transitions (e.g. $8 \rightarrow 7$ at 5290 Å in O^{5+} and C^{5+}) lie too close together to be resolved, we have selected instead a spectroscopic ‘window’ (about 8 Å wide) containing major Zeeman components of two prominent lines in the visible (multiplet 1, Table 1), emitted by C^{2+} and by O^+ , which permit adequate species resolution. Measured spectra are discussed and interpreted below.

Profile measurements were performed on the edge plasma of TEXTOR-94, in two independent observation directions: (i) in the equatorial plane tangentially to the magnetic flux surfaces (mainly σ_{\pm} components) with a plane grating (1200 grooves/mm, blaze angle 57°) Littrow spectrometer (S1, 3rd order); (ii) in the poloidal direction at right angles to the toroidal magnetic field (σ_{\pm} and/or π components) with an echelle grating (79 grooves/mm, blaze angle 76°) Littrow instrument (S2, 51st order, CCD with interference filter). While with S1, both wavelength (50 ms/spectrum) and radial (period 1 s) scans could be run simultaneously [1,6], S2 observed a fixed poloidal section of plasma (from minor radius $r = 49$ cm to 44 cm, covering part of a test limiter extending in to $r = 47$ cm) [2,7].

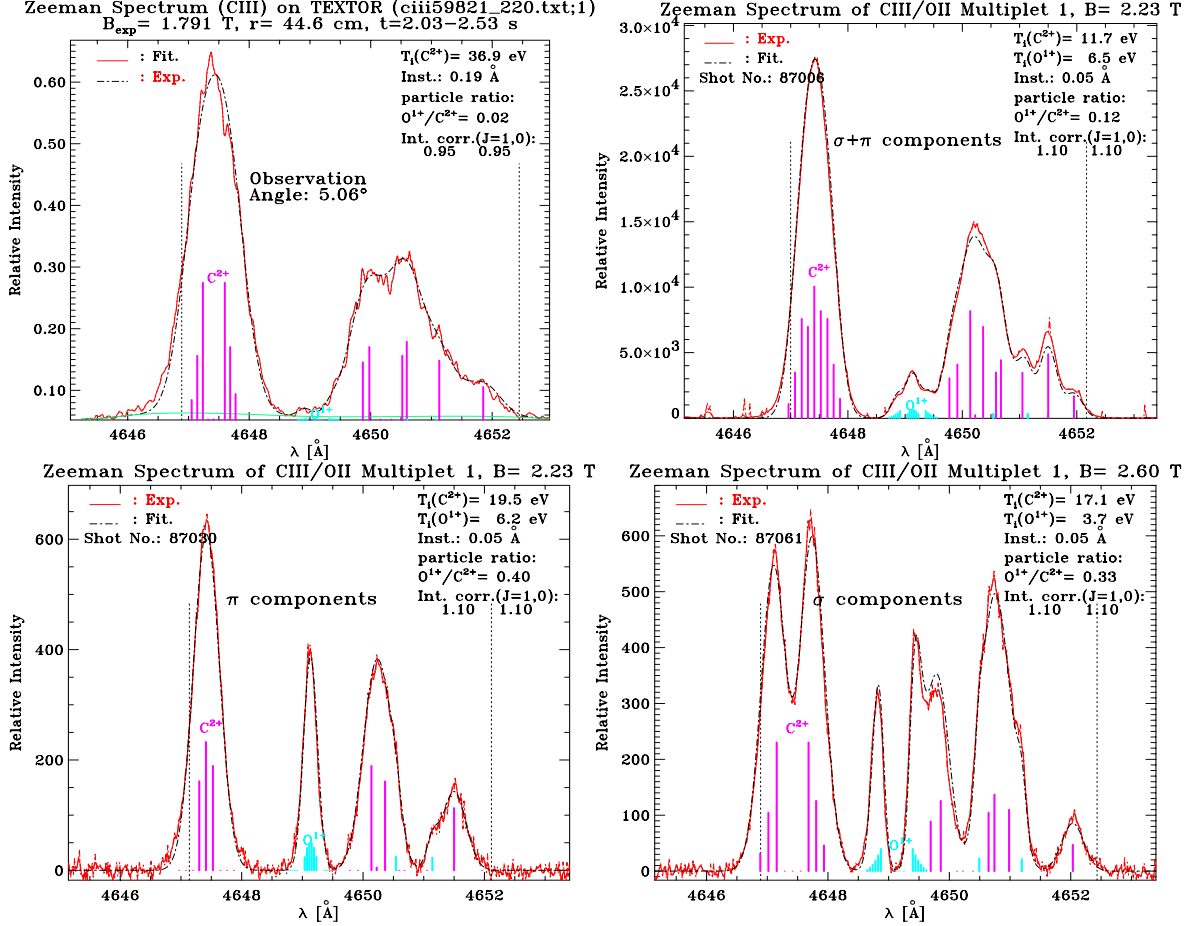
Table 1: The number of Zeeman components observed

C III: $2s 3p \ ^3P^o \rightarrow 2s 3s \ ^3S$			O II: $2p^2 \ (^3P) 3p \ ^4D^o \rightarrow 2p^2 3s \ ^4P$		
100 %	Components	allowed	48.3 %	Components	allowed
π	7	7	π	8	8
σ_{\pm}	12	12	σ_{\pm}	14	14

2. The role of the magnetic field and ion temperature determination

While the Paschen-Back effect [8-10] produces a significant perturbation of the line-strengths, it is ‘incomplete’ and hence the ‘diamagnetic’ quadratic Zeeman effect [10] need not be considered. A full treatment of the Paschen-Back effect is made for both triplet (C III) and quartet (O II) radiator systems in LS-coupling, by solving numerically for the eigenvalues and eigenfunctions of the appropriate tri-diagonal matrix [1,9,11], using

tabulations of the zero-field energy levels [12]. After unfolding the instrumental profile, ion temperatures are deduced from Doppler broadening of the individual Zeeman components by an IDL best-fit procedure with four fitting parameters [13], which finds (kT_C, kT_O) and the relative fractions of C^{2+} and O^+ within the chosen fitting range. Before fitting, a λ -dependent background is first subtracted. Examples of fitted profiles are shown in Fig. 1 (S1), Figs. 2-4 (S2), and corresponding data and results in Table 2.



Figs. 1-4: numbered consecutively from above left to right, below left to right.

Table 2: Some information on the discharges for which spectra are shown

Shot No.	I (kA)	$B(r)$ (T)	ΣP (MW)	\bar{n}_e (cm ⁻³)	$n_e(r)$ (cm ⁻³) (46 cm)	$kT_e(r)$ (eV) (47 cm)	$-\frac{d(kT_e)}{dr}$ (eV/cm)	kT_C (eV)	kT_O (eV)
59821	352	1.79	0.39	2.5 (13)	-	-	-	36.9	-
87006	398	2.23	2.57	5.7 (13)	6.5 (12)	25	5	11.7	6.5
87030	349	2.23	0.34	1.6 (13)	3.3 (12)	50	11	19.5	6.2
87061	387	2.60	0.34	3.4 (13)	3.2 (12)	37	15	17.1	3.7

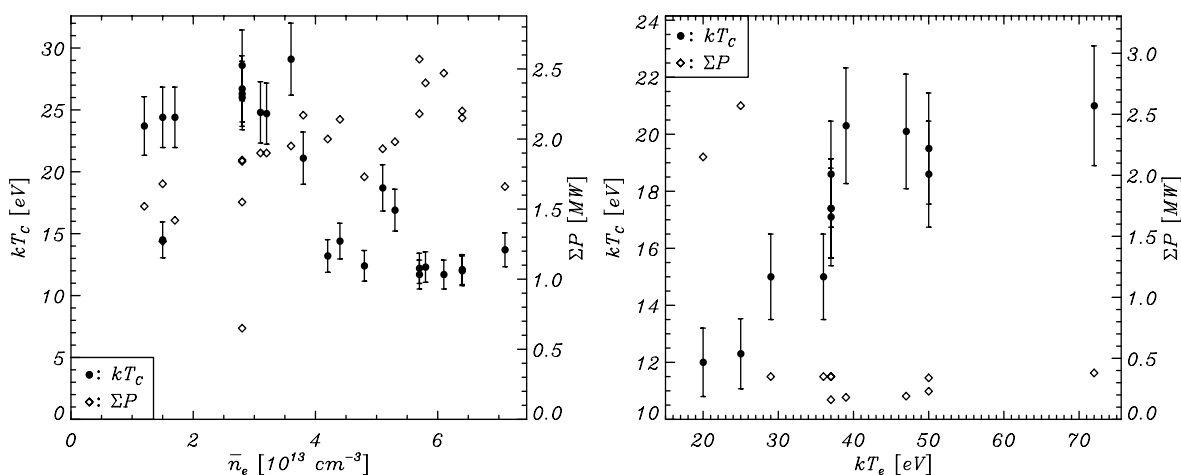
The symbols above each column denote: discharge no., current, local magnetic field-strength, total heating power, line averaged electron density, electron density at $r = 46$ cm, electron temperature at $r = 47$ cm, T_e gradient (for S2, averaged over the duration of spectral recording, 3s or 4s), C^{2+} temperature, O^+ temperature, respectively. Only the

second shot (87006) was heated by ICRH (0.86 MW) and neutral D double-beam injection (1.45 MW, hence neutron ‘spikes’ in Fig. 2). The remaining discharges were purely ohmic.

3. Interpretation: consideration of some important physical processes

Fitting of theoretical to measured profiles requires some assumption concerning the extent to which the upper fine-structure sublevel populations are ‘statistical’, i.e. whether ion collisions transfer population sufficiently rapidly *in the presence of the B-field* [13-15]. While the spectra from S1 indicate that the $J=2$ sublevels are slightly over-populated with respect to the $J=1,0$ sublevels (some 10-15 %), the reverse applies to the S2 spectra. The inference is that the S1 spectra have contributions from CXR of hotter C^{3+} ions; the S2 spectra, emitted from the vicinity of the test limiter, are excited only by electron collisions. The significantly higher S1 than S2 temperatures for C^{2+} support this distinction in origin.

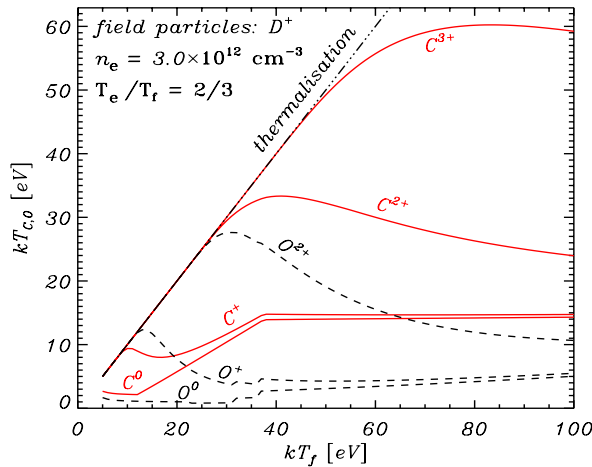
For a physical understanding of the respective temperatures of the two ion species C^{2+} and O^+ , in plasmas where the local values of T_e and T_i may differ significantly [1,16], we develop a model [1,17] based on ion collisional heating of *both* atomic and ion species [13,18]. Correlation data (Fig. 5) for D beam- and ICRH- heated D plasmas confirm the finding of Bogen and Rusbüldt [7,19], that physical sputtering dominates in the release of carbon atoms for $\bar{n}_e < 3.6 \cdot 10^{13} \text{ cm}^{-3}$, or equivalently, $kT_e > 30 \text{ eV}$.



Figs. 5-6: C^{2+} temperature as a function of average electron density \bar{n}_e and local T_e .

Data for mainly ohmically heated D plasmas with local values for n_e and T_e from He-beam diagnostics [20] tend to confirm this transition between chemical and physical sputtering regimes (Fig. 6, Table 2). In low- T_e edge plasmas, C^0 atoms are released with $kT_C \approx 1.5 \text{ eV}$, increasing to 13.5 eV for $kT_e \geq 25 \text{ eV}$ [19]. Ion collisional heating of these neutrals proceeds, prior to electron impact ionisation, through the charge-induced dipole interaction, for which the dipole polarisability is about $12a_0^3$, with a_0 =Bohr radius [13,18,21]. For O^0 the situation is very different, being mainly determined by chemical sputtering [7], or entirely by electron impact-induced dissociation of O_2 in those shots where the gas is admitted through the test limiter (Figs. 2-4). The latter process leaves one of the dissociated atoms in a quintet Rydberg state ($3s^5S^o, np^5P, 8 \leq n \leq 15$), and imparts a Franck-Condon energy/atom of 0.6, 1.0, or 2.0 eV and more for electron energies (roughly, kT_e) above 14.9 eV, 20.8 eV, 24.3 eV, respectively [22]. The dipole polarisability increases from about $5a_0^3$ to $63a_0^3$ in the metastable state, and then to huge values (above

$10^6 a_0^3$) for high n [13,18,21], but with corresponding dramatic decrease of the excited state lifetime with increasing n . After electron impact ionisation [23,24], ion heating [25] by



Coulomb collisions starts, and continues through each successive ionisation stage [1,17]. Important to note is the reduction in heating time through ionisation from excited (notably metastable) states [3,26]. With the aid of suitable rate coefficients for ground-state and excited state electron impact ionisation [26,27], curves such as Fig. 7 can be generated for typical ion to electron temperature ratios [16]. Their rich structure reflects the complexity of the atomic processes involved.

Fig. 7: Ion collisional heating of C and O atoms and ions in a deuterium plasma

4. Conclusion

Zeeman spectroscopy provides a valuable tool for impurity identification in edge plasmas, through determination of line positions, shapes and hence species temperatures.

REFERENCES

1. Hey J D, Lie Y T, Rusbüldt D, and Hintz E 1994 *Contrib. Plasma Phys.* **34** 725-747
2. Bogen P, Hey J D, Hintz E, *et al.* 1995 *J. Nucl. Mater.* **220-222** 472-477
3. Griem H R 1997 *Principles of Plasma Spectroscopy* (Cambridge U. P.)
4. Samm U, Bogen P, Claassen H A, *et al.* 1990 *J. Nucl. Mater.* **176-177** 273-277
5. Samm U *et al.* 1999 *Plasma Phys. Control. Fusion* **41** B57-B76
6. Hey J D *et al.* 1993 *Contr. Fus. Plasma Phys.* (20th EPS Lisbon) **17C** Part III 1111-1114
7. Bogen P and Rusbüldt D 1992 *J. Nucl. Mater.* **196-198** 179-183
8. Condon E U and Shortley G H 1951 *The Theory of Atomic Spectra* (Cambridge U. P.)
9. Kiess C C and Shortley G 1949 *J. Res. Nat. Bur. Stand.* **42** 183 – 207
10. Garstang R H 1977 *Rep. Prog. Phys.* **40** 105 – 154
11. Isler R C, Wood R W, Klepper C C, *et al.* 1997 *Phys. Plasmas* **4** 355 – 368
12. Wiese W L, Fuhr J R, and Deters T M 1996 *J. Phys. Chem. Ref. Data Monograph No. 7*
13. Hey J D, Chu C C, and Hintz E 1999 *J. Phys. B: At. Mol. Opt. Phys.* **32** 3555-3573
14. Hey J D, Korten M, Lie Y T, *et al.* 1996 *Contrib. Plasma Phys.* **36** 583-604
15. Bethe H A, Salpeter E 1957 *Quantum Mechanics of One- & 2 Electron Atoms* (Springer)
16. Huber A, Pospieszczyk A, *et al.* 2000 *Plasma Phys. Control. Fusion* **42** 569 – 578
17. McCracken G & Samm U 1992 *Proc. 8th Topic. Conf. At. Proc. Plasmas* 144-153 (AIP)
18. Hey J D, Chu C C, and Hintz E 2000 *Contrib. Plasma Phys.* **40** 9-22
19. Bogen P and Rusbüldt D 1992 *Nuclear Fusion* **32** 1057-1061
20. Brix M & Schweer B 1997 *Contr. Fus. Plasma Phys.* (24th EPS) **21A** Part IV 1837-1840
21. Mason E A and McDaniel E W 1988 *Transport Properties of Ions in Gases* (Wiley)
22. Freund R S 1971 *J. Chem. Phys.* **54** 3125-3141
23. Laher R R and Gilmore F R 1990 *J. Phys. Chem. Ref. Data* **19** 277-305
24. Jackman C H, Garvey R H, and Green A E S 1977 *J. Geophys. Res.* **82** 5081-5090
25. Spitzer, L Jr. 1962 *Physics of Fully Ionized Gases* (Interscience: New York)
26. Hey J D 1994 *Trans. Fusion Technol.* **25** (2T, Part 2) 315-325
27. Itikawa Y, Hara S, Kato T, *et al.* 1985 *Atom. Data Nucl. Data Tables* **33** 149-193